PPI Inhibitors

DOI: 10.1002/anie.201310082

Constrained Peptides with Target-Adapted Cross-Links as Inhibitors of a Pathogenic Protein–Protein Interaction**

Adrian Glas, David Bier, Gernot Hahne, Christoph Rademacher, Christian Ottmann, and Tom N. Grossmann**

Abstract: *Bioactive conformations of peptides can be stabilized by macrocyclization, resulting in increased target affinity and activity. Such macrocyclic peptides proved useful as modulators of biological functions, in particular as inhibitors of protein–protein interactions (PPI). However, most peptide-derived PPI inhibitors involve stabilized α-helices, leaving a large number of secondary structures unaddressed. Herein, we present a rational approach towards stabilization of an irregular peptide structure, using hydrophobic cross-links that replace residues crucially involved in target binding. The molecular basis of this interaction was elucidated by X-ray crystallography and isothermal titration calorimetry. The resulting cross-linked peptides inhibit the interaction between human adaptor protein 14-3-3 and virulence factor exoenzyme S. Taking into consideration that irregular peptide structures participate widely in PPIs, this approach provides access to novel peptide-derived inhibitors.*

Protein–protein interactions (PPI) contribute to virtually all aspects of cellular organization and function. The inhibition of PPIs allows the manipulation of biological processes and is considered a promising strategy towards next-generation therapeutics. PPIs often possess large interaction areas and lack well-defined binding pockets, which complicates the use of small-molecule inhibitors.[1] A promising alternative are peptide-based inhibitors that originate from a corresponding binding epitope.[2] However, such short linear peptide sequences tend to be highly flexible in solution and only adopt a defined three-dimensional structure upon binding. The restriction in conformational freedom associated with binding leads to entropic penalty,[3] resulting in an overall reduced affinity of the short peptide compared to its natural precursor. Preorganization of peptides into bioactive conformations can therefore increase binding affinity.[1a] The introduction of intramolecular cross-links is an appealing strategy to introduce such conformational constraint. Various cross-link architectures were reported to stabilize different secondary structures.[1a,4] Linear peptides have been cross-linked to provide classic cyclic and bicyclic peptides with improved bioactivity.[5] Moreover, β-sheets[6] and α-helices[4] have been rigidified by macrocyclization strategies. For the generation of PPI inhibitors, stabilization of α-helices by hydrogen-bond surrogates (HBS)[7] or cross-linked α-methylated amino acids (stapled peptides)[8] proved particularly useful.

The rational design of peptide-based PPI inhibitors is hampered by two major limitations: First, the utilized cross-links are generally neither designed nor optimized to interact with the binding partner. However, a few examples indicate that such cross-links have the potential to participate in target binding.[9] Second, most peptide-derived PPI inhibitors involve stabilized α-helices,[4] leaving a large fraction of interaction motifs unaddressed.[10] As a result, there is currently no rational approach for the stabilization of irregular peptide structures that frequently occur in PPI interfaces.[10] Herein, we present the structure-based design of constrained peptides that adopt an irregular structure when bound to their target. The constraining element is a hydrophobic cross-link evolved to directly interact with the protein target. These peptides inhibit the pathogenic interaction between virulence factor exoenzyme S (ExoS) and the human protein 14-3-3. Employing protein X-ray crystallography and isothermal titration calorimetry (ITC), we show in mechanistic detail how the cross-link contributes to protein binding, clearly rationalizing the structure–activity relationship of different linker lengths and configurations.

Our goal was the design of constrained peptides that are capable of inhibiting the ExoS–14-3-3 interaction. ExoS is a virulence factor of the pathogenic bacterium *Pseudomonas aeruginosa*, a major cause for infections associated with health care.[11] No current antibiotics are able to eradicate an established chronic infection involving multidrug-resistant strains.[12] Inhibition of the ExoS–14-3-3 interaction is considered a promising therapeutic strategy.[13] This PPI is mediated

[*] A. Glas,[+] D. Bier,[+] Dr. G. Hahne, Dr. T. N. Grossmann
Chemical Genomics Centre of the Max Planck Society
Otto-Hahn-Strasse 15, 44227 Dortmund (Germany)
E-mail: c.ottmann@tue.nl
tom.grossmann@cgc.mpg.de
Dr. C. Rademacher
Max-Planck-Institut für Kolloid- und Grenzflächenforschung
Am Mühlenberg 1, 14424 Potsdam (Germany)
Dr. C. Ottmann
University of Eindhoven, Department of Biomedical Engineering
Den Dolech 2, 5612 AZ Eindhoven (The Netherlands)
Dr. T. N. Grossmann
Technische Universität Dortmund, Fakultät für Chemie und chemische Biologie
Otto-Hahn-Strasse 6, 44227 Dortmund (Germany)
[+] Both authors contributed equally to this work.

[**] We thank C. Martin (Technical University of Dortmund) for performing high-resolution mass spectrometry; T.N.G. thanks the Fonds der Chemischen Industrie for financial support. The authors thank the German Research Foundation (DFG, Emmy Noether program RA1944/2-1 and GR3592/2-1).This work was supported by AstraZeneca, Bayer CropScience, Bayer HealthCare, Boehringer Ingelheim, Merck KGaA, and the Max Planck Society.

Supporting information for this article is available on the WWW under http://dx.doi.org/10.1002/anie.201310082.

by a peptide stretch of ExoS that binds 14-3-3 in an irregular conformation.[13] Previous studies indicate that eleven amino acids (^{420}QGLLDALDLAS^{430}, ESp) mainly contribute to binding.[13,14] We decided to use this ESp sequence as a starting point for the design of macrocyclic PPI inhibitors. To elucidate the exact binding mode of ESp, we synthesized an *N*-terminally acetylated version, which we co-crystallized with 14-3-3ζ (aa 1–230). Obtained crystals diffracted to 2.3 Å (PDB: 4N7G) allowing tracing of all amino acids (Figure 1a)

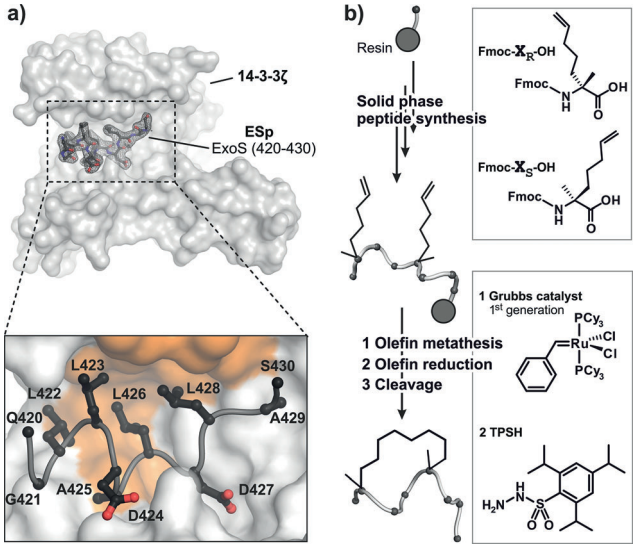

Figure 1. a) Top: Crystal structure of 14-3-3ζ in complex with ESp (sticks: C black, O red, N blue) with final $2F_o-F_c$ electron density (contoured at 1σ). Bottom: Closer view with interacting side chains of ESp shown explicitly. The hydrophobic patch on 14-3-3ζ is highlighted in orange (F117, P165, I166, G169, L172, L216, I217, L220). b) Synthetic route towards cross-linked peptides. Olefin-modified amino acids are introduced during solid-phase peptide synthesis followed by 1) cross-linking with ruthenium-mediated RCM, 2) Olefin reduction using TPSH; and 3) TFA cleavage (Fmoc: fluorenylmethyloxycarbonyl; TPSH: 2,4,6-triisopropylbenzenesulfonyl hydrazide).

of these crucial residues, we considered the use of olefin ring-closing metathesis (RCM) in analogy to the stapling of α-helical peptides.[8] This approach involves Fmoc-based solid-phase peptide synthesis (SPPS) using olefin bearing building blocks for the introduction of α-methyl, α-alkenyl non-natural amino acids (Figure 1b).[8] Subsequently, RCM is performed on solid support with first generation Grubbs catalyst. To avoid diastereomeric mixtures arising from the formation of *E*- and *Z*-configured double bonds, we decided to reduce the olefin using 2,4,6-triisopropylbenzenesulfonyl hydrazide (TPSH). Depending on the desired modification, the *N*-terminal amine was either capped with acetic anhydride or coupled with a polyethylene glycol (Peg) spacer and capped with fluorescein isothiocyanate (FITC). The corresponding fluorescein-modified peptides are indicated by the prefix "f".

Initially, we designed three peptides each equipped with two non-natural amino acids that are cross-linked by a $(CH_2)_8$ bridge (Figure 2a). One peptide ($\alpha_{SS}8$) bears two *S*-configured non-natural amino acids (X_S) at positions *i* and *i* + 4. The

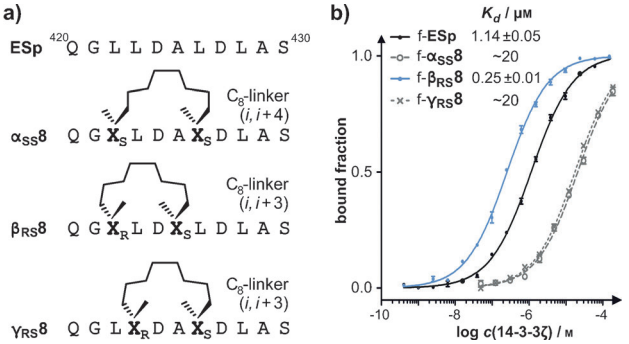

Figure 2. a) Modified peptides with three different cross-link architectures (α, β, γ); each with an eight carbon linker. Absolut configuration of α-methylated non-natural amino acids is indicated by subscript (X_R: R-configured, X_S: S-configured). b) FP assay of fluorescein-labeled peptides binding to full-length 14-3-3ζ (triplicate of runs, errors account for 1σ).

that superimpose almost perfectly (rmsd = 0.171 Å) with the corresponding residues of a previously reported longer ExoS fragment (Figures S8, S11).[13] ESp binds 14-3-3ζ in an irregular and mostly extended conformation, and with the exception of the *N*-terminal asparagine Q420 all residues are involved in 14-3-3ζ recognition. Crucial hydrophobic contacts are formed between a hydrophobic patch on 14-3-3ζ (orange, Figure 1a) and the core region of ExoS, encompassing four leucines (L422, L423, L426, L428) and an alanine (A425).

The elongated nature of ESp in the bound state renders a cyclization of *N* and *C* terminus, known from classic cyclic peptides, inappropriate for the installation of conformational constraint. Therefore, we inspected the peptide sequence for side chains that would allow the introduction of cross-links. Though strongly involved in protein recognition, we identified three pairs of hydrophobic residues (L422/L426, L422/A425, L423/L426) that are potentially suitable for cross-linking (Figure S12). To maintain the hydrophobic character

other two peptides (β- and γ_{RS}8) were modified with an *R*- and *S*-configured building block (X_R and X_S) at position *i* and *i* + 3, respectively (Figure 2a). The cross-linked peptides were investigated towards their binding affinities to 14-3-3 using fluorescence polarization (FP) as readout. The determined FP binding curves were used to calculate dissociation constants (K_d; Supporting Information, Figure S3), revealing a K_d of 1.14 μM for the interaction between f-ESp and 14-3-3ζ (Figure 2b). Cross-linked peptides f-α_{SS}8 and f-γ_{RS}8 exhibit an about 20-fold weaker binding to 14-3-3ζ ($K_d \approx 20$ μM). Notably, we observed a 4.6-fold increased affinity for f-β_{RS}8 ($K_d = 0.25$ μM) compared to starting sequence f-ESp. This is remarkable taking into consideration that the introduced cross-link replaces a leucine residue (L422), which was reported to be crucial for 14-3-3 binding.[13]

To understand the molecular basis of the β_{RS}8–14-3-3 interaction and to allow the design of more suitable cross-links, we co-crystallized β_{RS}8 with 14-3-3ζ (aa 1–230) and obtained crystals that diffracted to 2.1 Å (PDB: 4N7Y). The

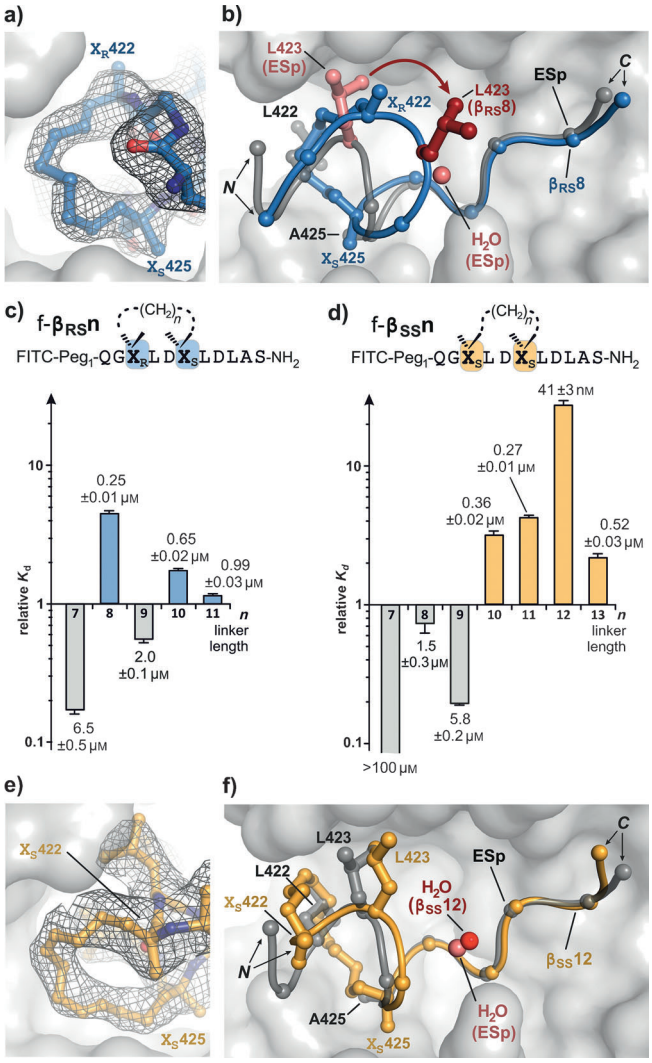

Figure 3. a) Final $2F_o-F_c$ electron density (contoured at 1σ) around the cross-link of $\beta_{RS}8$. b) Side view of superimposed structures of ESp (semitransparent gray) and $\beta_{RS}8$ (blue) in ribbon representation bound to 14-3-3ζ (gray surface). The cross-link and selected residues are shown in ball-and-stick representation. In ESp, L422 and A425 correspond to the cross-link positions in $\beta_{RS}8$ (N and C show peptide termini). c), d) Relative K_d values (K_d(f-ESp)/K_d(f-β_{RS}n)) derived from FP using fluorescein-labeled peptides and full-length 14-3-3ζ (triplicates, errors account for 1σ; for details, see the Supporting Information). e) Final $2F_o-F_c$ electron density (contoured at 1 s) around the cross-link of $\beta_{SS}12$. f) Side view of superimposed structures of ESp (semitransparent gray) and $\beta_{SS}12$ (orange) in ribbon representation bound to 14-3-3ζ (gray surface). Ball and stick representation in analogy to b).

electron density map for $\beta_{RS}8$ allows tracing of the entire molecule, including the hydrophobic cross-link, which is intimately involved in interactions with non-polar residues of 14-3-3ζ (Figure 3a; Figures S13, S14). A comparison of $\beta_{RS}8$ and ESp in complex with 14-3-3ζ reveals the same binding site for both peptides (Figure 3b). Notably, the *N*-terminal part of the backbone in $\beta_{RS}8$ is rearranged compared to ESp, resulting in the loss of direct as well as water-mediated polar interactions. Most obviously, a water molecule (red, Figure 3b) that is involved in hydrogen bonds with backbone atoms of ESp is absent in the structure of $\beta_{RS}8$ (Figure S16). Furthermore, a dislocation of the crucial leucine residue L423 (red, Figure 3b) is observed and leads to a complete absence of hydrophobic contacts between L423 of $\beta_{RS}8$ and 14-3-3ζ. To further improve peptide binding, we considered the evolution of the cross-link focusing on both the cross-link length and the absolute configuration of the non-natural amino acids. For the generation of a small peptide library, $\beta_{RS}8$ (linker length: $n=8$) was used as starting point. First, a set of peptides with the same configuration as $\beta_{RS}8$ (*R* at position 422 and *S* at position 425) but varied linker length was synthesized ($n=7$–11). Fluorescein-labeled versions of these peptides were tested regarding their affinity for 14-3-3ζ using FP (Figure 3c). Installation of a shortened cross-link ($n=7$; $K_d=6.5$ μM) resulted in dramatically reduced binding affinity. Interestingly, longer linkages ($n=9$–11) did not improve binding either ($K_d=0.65$–2.0 μM), revealing $\beta_{RS}8$ ($K_d=0.25$ μM) as the most suitable cross-link in this series.

Next, we considered a variation of the absolute configuration of both non-natural amino acids. Inspection of the $\beta_{RS}8$–14-3-3ζ structure (Figure 3a) indicates a strong engagement of X_S425 in 14-3-3ζ binding, rendering this position less suitable for further modifications. However, the Cα-centered portion of X_R422 shows little direct involvement in binding, and thus was selected for modification. A set of peptides with two *S*-configured non-natural amino acids ($\beta_{SS}n$) and linker lengths ranging from 7 to 13 was synthesized. FP measurements revealed a strong dependence of their binding affinity to 14-3-3ζ on the linker length (Figure 3d). In this series, longer cross-links containing 10 to 13 carbon atoms provide the most affine peptides with significant increases in affinities (2- to 28-fold) compared to the unmodified sequence ESp. Peptide f-$\beta_{SS}12$ is the most affine 14-3-3ζ binder ($K_d=41$ nM), exhibiting a sixfold higher affinity than f-$\beta_{RS}8$ and a 28-fold higher affinity than f-ESp. To elucidate the structural consequences of the altered cross-link architecture in $\beta_{SS}12$, we crystallized the peptide in complex with 14-3-3ζ (aa 1–230) and determined the structure at a resolution of 2.5 Å (PDB: 4N84). The hydrophobic cross-link is clearly traced (Figure 3e) and again involved in interactions with hydrophobic residues of 14-3-3ζ (Figure S18). In contrast to $\beta_{RS}8$, the arrangement of the backbone in $\beta_{SS}12$ is very similar to the unmodified peptide ESp resulting in an almost identical interaction of 14-3-3ζ, with leucine L423 in $\beta_{SS}12$ and in ESp (Figure 3f). Similar to ESp, the backbone of $\beta_{SS}12$ coordinates a water molecule that is absent in $\beta_{RS}8$ (red, Figure 3b,f; Figure S20).

To validate the FP measurements and to gain a more detailed understanding of the thermodynamics of the binding process, ITC experiments with 14-3-3ζ in presence of acetylated peptides were performed. In accordance to FP, $\beta_{SS}12$ proved to be the most affine binder ($K_d=0.15$ μM) showing a 3.7- and 15-fold stronger binding than $\beta_{RS}8$ ($K_d=0.55$ μM) and ESp ($K_d=2.2$ μM), respectively (Figure 4a). A comparison of enthalpic (ΔH, white) contributions to the free enthalpy of binding (ΔG, gray) at 303 K shows the smallest ΔH upon binding for $\beta_{RS}8$ (-4.0 kcal mol^{-1}). This is in agreement with the dislocation of the *N*-terminal part and the resulting lack in polar interactions with 14-3-3ζ (Fig-

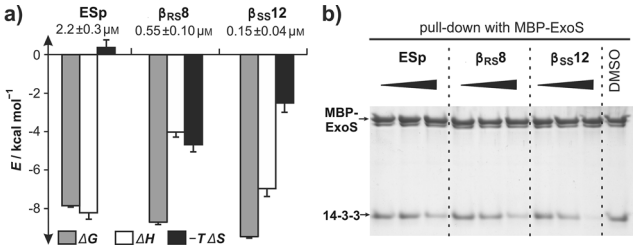

Figure 4. a) Comparison of ITC-derived enthalpy (ΔH, white) and entropic contribution ($-T\Delta S$, black) to the free binding enthalpy (ΔG, gray) at 303 K (30 °C). b) In vitro competition of ESp, $\beta_{RS}8$, and $\beta_{SS}12$ with an *N*-terminally MBP-tagged ExoS fragment, including amino acids 355–453 (MBP-ExoS) for 14-3-3ζ (aa 1–230) binding. The MBP-ExoS-14-3-3ζ complex (2 μM) was incubated with increasing amounts of peptide (2, 10, 50 μM) for 2 h. DMSO served as control. Amylose resin was used for pull-down. After washing, bound proteins were separated by SDS-PAGE and visualized by Coomassie staining.

ure 3b). ESp and $\beta_{SS}12$ on the other hand establish similar interactions with 14-3-3ζ, explaining their comparable binding enthalpy (−8.2 and −7.0 kcal mol^{-1}). The binding of ESp to 14-3-3ζ exhibits negligible contributions by $-T\,\Delta S$ (black). This indicates that favorable entropic contributions like the liberation of water molecules (classic hydrophobic effect) on the one hand and entropic penalties such as restriction in conformational freedom on the other appear to be approximately balanced. Compared to ESp, both cross-linked peptides show significantly improved entropic contributions ($-T\,\Delta S = -4.7$ for $\beta_{RS}8$ and −2.5 kcal mol^{-1} for $\beta_{SS}12$) leading to their increased affinity.

A possible explanation for the improved binding entropy is a cross-link-induced restriction of conformational freedom of the free peptide, resulting in reduced entropic penalty upon binding. To test this hypothesis, we investigated the structural characteristics of these peptides in solution. First, we performed circular dichroism (CD) spectroscopy of the unbound peptides. These measurements did not show a pronounced secondary structure for any of the peptides but indicate a reduced content of flexible random coil structures for the cross-linked sequences $\beta_{RS}8$ (49%) and $\beta_{SS}12$ (51%) compared to ESp (61%; Table S8). Second, we determined ^{1}H-nuclear magnetic resonances (NMR) of backbone amides (-CO-N*H*-), which are a good indication for defined backbone structures in peptides. Usually, more rigid peptides exhibit larger dispersion in their ^{1}HN chemical shifts than their flexible analogues. We analyzed the ^{1}HN resonances in a buffered aqueous solution (10% D_2O) at pH 6.3 (Figure S23). The ^{1}HN backbone chemical shifts recorded for the unmodified peptide ESp at 288 K show a relative low dispersion of ±0.18 ppm (average chemical shift: $\delta =$ 8.27 ppm). This indicates a conformational flexibility that averages the contributions from dipolar interactions and is close to a value expected for ^{1}HN shifts in random coils.[15] In contrast, ^{1}HN resonances of $\beta_{RS}8$ and $\beta_{SS}12$ are more disperse with values of ±0.31 and ±0.37 ppm, respectively (average chemical shifts: $\delta = 8.10$ and 8.14 ppm). These findings indicate a reduction of conformational flexibility. This interpretation should be made cautiously as it cannot be ruled out that changes in the chemical environment introduced by the cross-link could result in similar phenomena. However, in combination with the reduction of random coil structures (CD measurements) and the increase in binding entropy (ITC) for $\beta_{RS}8$ and $\beta_{SS}12$, these results suggest a decrease of conformational flexibility upon cross-link incorporation.

The introduction of hydrophobic cross-links provided peptides with significantly enhanced binding affinities for 14-3-3ζ. Knowing that the interaction between virulence factor ExoS and human 14-3-3 is a potential antibiotic target, we were interested in the capability of the peptides to inhibit this PPI. An in vitro pull-down assay was employed using 14-3-3ζ (aa 1–230) and a fragment of ExoS (aa 355–453) tagged with maltose-binding protein (MBP-ExoS). The complex between 14-3-3ζ and MBP-ExoS was incubated with peptides ESp, $\beta_{RS}8$, and $\beta_{SS}12$, respectively. Thereafter, amylose resin was used to immobilize MBP-ExoS, and after washing, bound proteins were analyzed by gel electrophoresis (Figure 4b). The gel shows that the pull-down of 14-3-3ζ is reduced in presence of $\beta_{RS}8$ and $\beta_{SS}12$ in a dose-dependent manner. The inhibitory efficiency for the 14-3-3ζ–ExoS interaction correlates well with obtained binding affinities, showing the most efficient competition for the best binder $\beta_{SS}12$.

In summary, we introduce a strategy for the macrocyclization of bioactive peptides with an irregular secondary structure by utilizing cross-links explicitly designed to be involved in target binding. As a proof of concept, we target the complex between the human adaptor protein 14-3-3 and virulence factor ExoS, which is considered an attractive antibiotic strategy.[13] Using the interaction motif of ExoS as starting point, we developed a macrocyclic molecule with a circa 20-fold increased affinity for 14-3-3 and the ability to efficiently inhibit its interaction with ExoS in vitro. The final and unique cross-link architecture was evolved in a rational and iterative process that should be applicable to a broad range of irregular peptide structures. Taking into consideration that irregular structures participate widely in PPIs,[10] our approach is an appealing strategy for the generation of novel peptide-derived inhibitors. Moreover, the development of macrocyclic interaction motifs can foster the rational design of peptidomimetics,[4,16] combining the surface recognition properties of peptides and the pharmacological behavior of small molecules.

Received: November 20, 2013
Published online: February 6, 2014

Keywords: cyclic peptides · hydrophobic cross-links · protein–protein interactions · *Pseudomonas aeruginosa* · ring-closing metathesis

[1] a) A. J. Wilson, *Chem. Soc. Rev.* **2009**, *38*, 3289 – 3300; b) P. Thiel, M. Kaiser, C. Ottmann, *Angew. Chem.* **2012**, *124*, 2052 – 2059; *Angew. Chem. Int. Ed.* **2012**, *51*, 2012 – 2018.
[2] N. London, B. Raveh, D. Movshovitz-Attias, O. Schueler-Furman, *Proteins Struct. Funct. Bioinf.* **2010**, *78*, 3140 – 3149.
[3] K. N. Houk, A. G. Leach, S. P. Kim, X. Y. Zhang, *Angew. Chem.* **2003**, *115*, 5020 – 5046; *Angew. Chem. Int. Ed.* **2003**, *42*, 4872 – 4897.

[4] V. Azzarito, K. Long, N. S. Murphy, A. J. Wilson, *Nat. Chem.* **2013**, *5*, 161 – 173.
[5] a) C. J. White, A. K. Yudin, *Nat. Chem.* **2011**, *3*, 509 – 524; b) M. Katsara, T. Tselios, S. Deraos, G. Deraos, M.-T. Matsoukas, E. Lazoura, J. Matsoukas, V. Apostolopoulos, *Curr. Med. Chem.* **2006**, *13*, 2221 – 2232; c) A. Angelini, L. Cendron, S. Y. Chen, J. Touati, G. Winter, G. Zanotti, C. Heinis, *ACS Chem. Biol.* **2012**, *7*, 817 – 821.
[6] J. A. Robinson, *Acc. Chem. Res.* **2008**, *41*, 1278 – 1288.
[7] A. Patgiri, M. Z. Menzenski, A. B. Mahon, P. S. Arora, *Nat. Protoc.* **2010**, *5*, 1857 – 1865.
[8] Y. W. Kim, T. N. Grossmann, G. L. Verdine, *Nat. Protoc.* **2011**, *6*, 761 – 771.
[9] a) S. Baek, P. S. Kutchukian, G. L. Verdine, R. Huber, T. A. Holak, K. W. Lee, G. M. Popowicz, *J. Am. Chem. Soc.* **2012**, *134*, 103 – 106; b) M. L. Stewart, E. Fire, A. E. Keating, L. D. Walensky, *Nat. Chem. Biol.* **2010**, *6*, 595 – 601; c) C. Phillips, L. R. Roberts, M. Schade, R. Bazin, A. Bent, N. L. Davies, R. Moore, A. D. Pannifer, A. R. Pickford, S. H. Prior, C. M. Read, A. Scott, D. G. Brown, B. Xu, S. L. Irving, *J. Am. Chem. Soc.* **2011**, *133*, 9696 – 9699; d) Y. S. Chang, B. Graves, V. Guerlavais, C. Tovar, K. Packman, K.-H. To, K. A. Olson, K. Kesavan, P. Gangurde, A. Mukherjee, T. Baker, K. Darlak, C. Elkin, Z. Filipovic, F. Z. Qureshi, H. L. Cai, P. Berry, E. Feyfant, X. G. E. Shi, J. Horstick, D. A. Annis, A. M. Manning, N. Fotouhi, H. Nash, L. T. Vassilev, T. K. Sawyer, *Proc. Natl. Acad. Sci. USA* **2013**, *110*, E3445 – E3454.
[10] M. Guharoy, P. Chakrabarti, *Bioinformatics* **2007**, *23*, 1909 – 1918.
[11] G. M. Rossolini, E. Mantengoli, *Clin. Microbiol. Infect.* **2005**, *11*, 17 – 32.
[12] a) G. H. Talbot, J. Bradley, J. E. Edwards, D. Gilbert, M. Scheld, J. G. Bartlett, *Clin. Infect. Dis.* **2006**, *42*, 657 – 668; b) N. Srinivas, P. Jetter, B. J. Ueberbacher, M. Werneburg, K. Zerbe, J. Steinmann, B. Van der Meijden, F. Bernardini, A. Lederer, R. L. A. Dias, P. E. Misson, H. Henze, J. Zumbrunn, F. O. Gombert, D. Obrecht, P. Hunziker, S. Schauer, U. Ziegler, A. Kaech, L. Eberl, K. Riedel, S. J. DeMarco, J. A. Robinson, *Science* **2010**, *327*, 1010 – 1013; c) A. Bernardi, J. Jiménez-Barbero, A. Casnati, C. De Castro, T. Darbre, F. Fieschi, J. Finne, H. Funken, K.-E. Jaeger, M. Lahmann, T. K. Lindhorst, M. Marradi, P. Messner, A. Molinaro, P. V. Murphy, C. Nativi, S. Oscarson, S. Penades, F. Peri, R. J. Pieters, O. Renaudet, J.-L. Reymond, B. Richichi, J. Rojo, F. Sansone, C. Schaeffer, W. B. Turnbull, T. Velasco-Torrijos, S. Vidal, S. Vincent, T. Wennekes, H. Zuilhof, A. Imberty, *Chem. Soc. Rev.* **2013**, *42*, 4709 – 4727.
[13] C. Ottmann, L. Yasmin, M. Weyand, J. L. Veesenmeyer, M. H. Diaz, R. H. Palmer, M. S. Francis, A. R. Hauser, A. Wittinghofer, B. Hallberg, *EMBO J.* **2007**, *26*, 902 – 913.
[14] L. Yasmin, J. L. Veesenmeyer, M. H. Diaz, M. S. Francis, C. Ottmann, R. H. Palmer, A. R. Hauser, B. Hallberg, *Biochem. J.* **2010**, *427*, 217 – 224.
[15] a) C. C. McDonald, W. D. Phillips, *J. Am. Chem. Soc.* **1967**, *89*, 6332 – 6341; b) R. Page, W. Peti, I. A. Wilson, R. C. Stevens, K. Wuthrich, *Proc. Natl. Acad. Sci. USA* **2005**, *102*, 1901 – 1905.
[16] E. Ko, J. Liu, K. Burgess, *Chem. Soc. Rev.* **2011**, *40*, 4411 – 4421.

